



ELSEVIER

Neurocomputing 32–33 (2000) 113–119

---

---

NEUROCOMPUTING

---

---

www.elsevier.com/locate/neucom

# A combined computational and intracellular study of correlated synaptic bombardment in neocortical pyramidal neurons in vivo

Alain Destexhe\*, Denis Paré

*Department of Physiology, Laboratory of Neurophysiology, Laval University, Pavillon Vandry, Québec, Canada G1K 7P4*

Accepted 13 January 2000

---

## Abstract

Computational models and intracellular recordings were combined to characterize synaptic bombardment in neocortical pyramidal neurons during active states in vivo. Application of tetrodotoxin revealed that synaptic activity accounts for up to 80% of the input conductance. These experiments were replicated assuming that excitatory and inhibitory synapses release randomly at high rates (1–5 Hz). A significant correlation between synaptic events had to be introduced to account for the membrane potential fluctuations recorded experimentally. We conclude that pyramidal neurons in vivo experience high-frequency synaptic events with a significant correlation. The consequences of this synaptic bombardment on cellular responsiveness are investigated in the companion paper. © 2000 Elsevier Science B.V. All rights reserved.

*Keywords:* Cerebral cortex; Dendritic integration; Synaptic background activity; Computational models; Arousal

---

## 1. Introduction

The synaptic connectivity of the neocortex is very dense, each pyramidal cell receiving 5000 to 60,000 synapses [3], 70% of which originate from other cortical neurons. Given that neocortical neurons spontaneously fire at 5–20 Hz in awake

---

\* Corresponding author. Present address: UNIC, Institut de Neurobiologie Alfred Fessard, CNRS, Avenue de la Terrasse, 91128 Gif-sur-Yvette, France. Tel.: + 00-1-418-656-5711; fax: + 00-1-418-656-7898.  
*E-mail address:* alain@fmed.ulaval.ca (A. Destexhe).

animals [9,15], cortical cells must experience tremendous synaptic currents. This synaptic background activity (also called *synaptic bombardment*) may significantly influence the integrative properties of cortical neurons.

This theme was explored by several modeling studies on cortical [1,7,13], thalamic [4] and cerebellar neurons [19,24]. These models predicted that the dendritic conductances tonically activated by background activity profoundly affect the electrotonic properties of neurons as well as their firing behavior. Unfortunately, few experiments are available to constrain synaptic bombardment because of the technical difficulty of performing intracellular recordings in awake animals.

To characterize synaptic background activity, our approach [7] has been to combine computational models of neocortical pyramidal neurons with *in vivo* intracellular data obtained in ketamine–xylazine anesthetized cats before and after local microperfusion of tetrodotoxin (TTX) or synaptic blockers [16,18]. The interest of this approach derives from the fact that ketamine–xylazine anesthetized animals display spontaneous periods of desynchronized electroencephalogram (EEG) activity, with cortical neurons firing spontaneously at 5–20 Hz, which are features similar to the waking state [21,22]. Thus, using this paradigm, we estimated the release conditions during active states associated to desynchronized EEG, as we report here.

## 2. Experimental characterization of active states

Intracellular recordings of morphologically identified pyramidal neurons were performed in cat neocortex (area 5–7) during ketamine–xylazine anesthesia. An array of stimulating tungsten electrodes and a microperfusion pipette were inserted in cortex, and intracellular recordings were obtained in their vicinity (1–2 mm; see Methods in Refs. [16–18]). Active periods were selected based on the following criteria: (a) the EEG is desynchronized; (b) the cell fires tonically in the 5–20 Hz range; (c) the period is long enough ( $> 1$  s) to allow analysis.

To estimate the effect of network activity, we have compared intracellularly recorded cells in active periods and after microperfusion of TTX to the cortex. During active periods, neocortical neurons were characterized by highly fluctuating activity and spontaneous firing in the 5–20 Hz range (Fig. 1A1). After microperfusion of TTX, this activity was abolished (Fig. 1A2) and responses to cortical stimulation were totally suppressed [16,18].

The input resistance ( $R_{in}$ ) was estimated before and after TTX application by injection of hyperpolarizing current pulses in the linear portion of current–voltage relations. During active states, neocortical neurons had a low  $R_{in}$  ( $9.2 \pm 4.3$  M $\Omega$ ; mean  $\pm$  SE;  $n = 26$ ), as shown by the relatively small-voltage responses to intracellular current injection (Fig. 1B1). After TTX, the same cells showed a much larger  $R_{in}$  ( $46 \pm 8$  M $\Omega$ ;  $n = 9$ ), calculated at the same  $V_m$  (Fig. 1B2). Although the absolute  $R_{in}$  values varied from cell to cell, 9 cells recorded before and after TTX showed similar *relative* changes, showing a five-fold ( $81.4 \pm 3.6\%$ )  $R_{in}$  decrease during active periods compared to quiescent conditions.

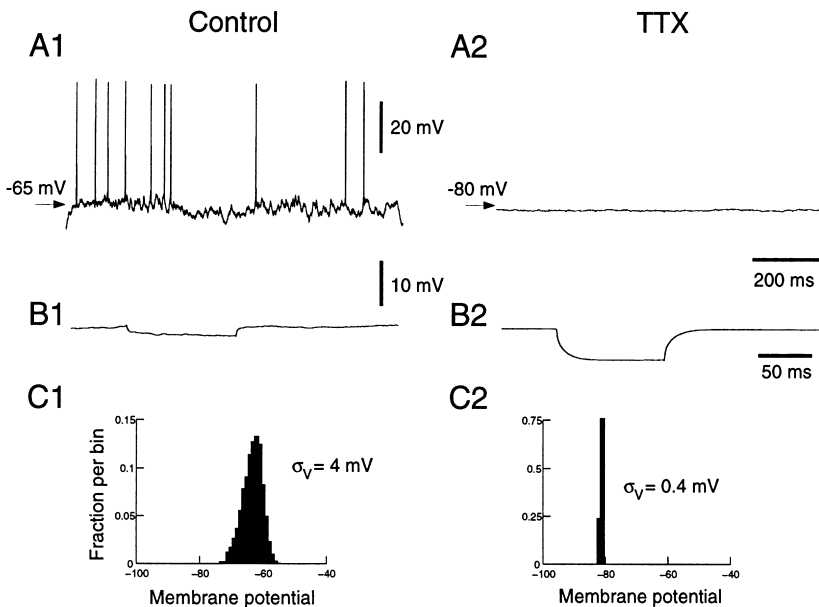


Fig. 1. Electrophysiological characteristics of neocortical pyramidal neurons during active states. (A) Intracellular recording of a neocortical neuron in cat parietal cortex (area 5–7) during a phase of desynchronized EEG activity (ketamine–xylazine anesthesia). The same neuron is shown before (A1) and after (A2) microperfusion of TTX, abolishing all spontaneous activity. (B) Average of 50 hyperpolarizing pulses ( $-0.1$  nA) to estimate the input resistance, during active periods (B1) and after TTX (B2). (C) Distribution of membrane potential before (C1) and after TTX (C2). TTX abolished most membrane potential ( $V_m$ ) fluctuations, increased the  $R_{in}$  by about five-fold, and hyperpolarized the cell by about 15 mV.

Another aspect of background activity is that cortical neurons display high-amplitude  $V_m$  fluctuations (Fig. 1A1). Measuring the amplitude of fluctuations by calculating the standard deviation of the  $V_m$  ( $\sigma_v$ ) revealed that, in 9 different cells recorded successively during active periods and after TTX application,  $\sigma_v$  was reduced from  $4.0 \pm 2.0$  to  $0.4 \pm 0.1$  mV, respectively, as illustrated by histograms of  $V_m$  distribution (Fig. 1C). These histograms also show that, after TTX, the  $V_m$  dropped significantly to  $-80 \pm 2$  mV, as reported previously [18]. During active periods, the average  $V_m$  was  $-65 \pm 2$  mV in control conditions (K-Acetate-filled pipettes) and  $-51 \pm 2$  mV with chloride-filled recording pipettes. These conditions correspond to chloride reversal potentials ( $E_{Cl}$ ) of  $-73.8 \pm 1.6$  and  $-52.0 \pm 2.9$  mV, respectively [17].

Taken together, these data show that active periods are characterized by (a) a  $\sim 5$ -fold decrease in  $R_{in}$ ; (b) a significant depolarization of 15–30 mV depending on the recording conditions; (c) a  $\sim 10$ -fold increase in the amplitude of  $V_m$  fluctuations. In the following, we use computational models to estimate the release conditions at glutamatergic and GABAergic synapses to account for these data.

### 3. Computational models of active states

Computational models were based on four morphologically reconstructed pyramidal neurons from cats (one from layer II–III, two from layer V and one from layer VI), which were obtained from two previous studies [2,8]. Simulations obtained using layer VI pyramidal cell (Fig. 2A) are shown here, but these results were robust to changes in the dendritic morphology and were therefore not dependent on the specific cell used (see details in Ref. [7]). Voltage-dependent conductances were inserted in soma, dendrites and axon.  $\text{Na}^+$  and  $\text{K}^+$  currents were simulated by Hodgkin and Huxley [11] type models, and had kinetics and soma/dendrite densities based on measurements in hippocampal or neocortical pyramidal neurons (see details in Ref. [7]). Synaptic currents were simulated by kinetic models of glutamatergic and GABAergic receptors: glutamate  $\alpha$ -amino-3-hydroxy-5-methyl-4-isoxazolepropionic acid (AMPA), glutamate N-methyl-D-aspartate (NMDA), and  $\gamma$ -aminobutyric acid type-A ( $\text{GABA}_A$ ) receptor types were simulated according to two-state kinetic models

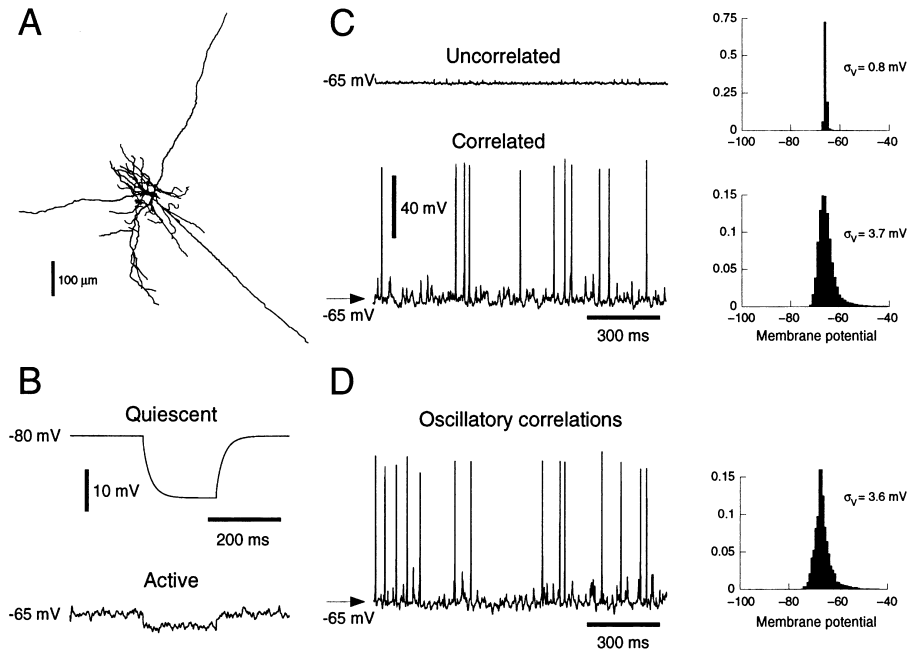


Fig. 2. Model of neocortical pyramidal neurons during active states. (A) Reconstructed layer VI pyramidal neuron used for simulations. (B) Injection of hyperpolarizing current in the presence (active) and in the absence (quiescent) of synaptic bombardment (C) *Uncorrelated*: random synaptic events at high frequency produced correct  $R_{in}$  and average  $V_m$ , but almost no  $V_m$  fluctuations because of the large number of random events. *Correlated*: introducing a constant correlation ( $c = 0.1$ ) between synaptic events led to correct  $V_m$  fluctuations and spontaneous firing, similar to intracellular recordings. (D) Model similar to C, with correlations oscillating between 0 and 0.2 at 40 Hz.  $V_m$  distributions are indicated on the right for C and D.

[5,6]. The densities of synapses in different regions of the cell were estimated from morphological studies in neocortical pyramidal cells [3] (see details in Ref. [7]). The number of synapses per  $100 \mu\text{m}^2$  of membrane were: 10–20 ( $\text{GABA}_A$ , soma), 40–80 ( $\text{GABA}_A$ , axon initial segment), 8–12 ( $\text{GABA}_A$ , dendrites) and 55–65 (AMPA-NMDA, dendrites), leading to a total of 16 563 glutamatergic and 3376  $\text{GABA}_A$ ergic synapses for the layer VI cell shown in Fig. 2A. Using these synapse densities, quantal conductances were estimated by matching the model to recordings of miniature synaptic events [7] and were 1200 ps for AMPA and 600 ps for  $\text{GABA}_A$ .

The interest of the present approach is that the model could be constrained by recordings of the same neurons during three different states: active periods with desynchronized EEG (see above), miniature synaptic events (microperfusion of TTX) and absence of synaptic activity (TTX + synaptic blockers). To characterize active periods, the model was constrained according to the following steps (see details in Ref. [7]): (1) the passive properties were estimated based on recordings in the absence of synaptic activity; (2) quantal conductances and synaptic densities were estimated from miniature synaptic events; (3) active periods were modeled based on the assumption that they are generated by the same populations of synapses that produced miniature events, except that the release frequency is higher. Assuming that quantal conductances and release frequencies are uniform, the same model could reproduce the following experimental measurements: (a) neocortical neurons have a high  $R_{\text{in}}$  and hyperpolarized rest in quiescent conditions (Fig. 1A2, B2); (b) in the presence of synaptic bombardment, the  $R_{\text{in}}$  is about five-fold lower (Fig. 1B) and the  $V_m$  is depolarized by about 15 mV (Fig. 1C); (c) with IPSPs reversed around  $-55$  mV, the  $V_m$  depolarizes further by about 10–15 mV (not shown). This model is illustrated in Fig. 2B.

Thus, several features of active states can be modeled assuming that pyramidal neurons receive random synaptic events corresponding to high release frequencies, namely 1 Hz for AMPA-mediated synapses and 5.5 Hz for  $\text{GABA}_A$ -mediated synapses (compared to 0.009–0.012 Hz for miniature events). Several combinations of parameters were consistent with experimental data, but the domain of these parameters was narrow (see details in [7]).

At this point, the model accounts for the  $R_{\text{in}}$  and average  $V_m$  recorded experimentally. However, due to the large number of synaptic events occurring randomly, the membrane was virtually clamped around  $-65$  mV (Fig. 2C, uncorrelated). A search for the effect of various parameters, such as quantal conductances, release frequency and synapse density, always produced too small amplitudes of  $V_m$  fluctuations [7]. However, introducing a correlation ( $c = 0.1$ ) between the different release events produced fluctuations of larger amplitude (Fig. 2C, correlated), leading to spontaneous firing and amplitude distributions consistent with experimental data (Fig. 2C, right panels).

These results were checked with four cell geometries [7]. Considering the same values of conductance density (both passive and synaptic), different cells showed different absolute values of  $R_{\text{in}}$ , but all showed similar *relative*  $R_{\text{in}}$  changes of about 80%, similar to experiments (see details in [7]). For all cells, a significant correlation was necessary to yield correct values of  $\sigma_v$ .

Finally, because active states are characterized by marked oscillatory activity in the fast (20–60 Hz) frequency range [20], we also considered the case of oscillatory correlations. Instead of using random events occurring with a constant correlation of  $c = 0.1$ , the release at different synapses still was random, but was correlated according to a sinusoidal temporal pattern (correlation oscillating between 0 and 0.2 with a period of 25 ms). This oscillatory pattern of correlation produced large-amplitude  $V_m$  fluctuations with correct  $R_{in}$ ,  $\sigma_v$  and average  $V_m$  (Fig. 2D). This case was therefore indistinguishable from the constant correlation case, except that oscillatory components are enhanced (compare C and D in Fig. 2), which is a feature often seen in intracellularly recorded cells during active states.

#### 4. Conclusion

In conclusion, this combination of computational models with in vivo intracellular recordings suggests that during active states with desynchronized EEG activity, as in the wake state, pyramidal neurons are subject to important currents mostly of synaptic origin, in agreement with previous reports [7,10,18]. This synaptic bombardment accounts for up to 80% of the input conductance, which is in the upper range of previous theoretical estimates [1,13]. Perhaps the most surprising result was that a significant correlation between individual release events had to be introduced. This correlation may be due to the fact that in the cortex, single axons usually establish several synaptic contacts per cell [14,23]. Also, the presence of oscillatory amplitude fluctuations in the EEG implies correlated activity in the network. The consequences of this type of synaptic activity on cellular responsiveness are investigated in the companion paper [12].

#### Acknowledgements

Research supported by grants from the Medical Research Council of Canada and the National Institutes of Health (R01-NS37711).

#### References

- [1] O. Bernander, R.J. Douglas, K.A. Martin, C. Koch, Synaptic background activity influences spatiotemporal integration in single pyramidal cells, *Proc. Natl. Acad. Sci. USA* 88 (1991) 11 569–11 573.
- [2] D. Contreras, A. Destexhe, M. Steriade, Intracellular and computational characterization of the intracortical inhibitory control of synchronized thalamic inputs in vivo, *J. Neurophysiol* 78 (1997) 335–350.
- [3] J. DeFelipe, I. Fariñas, The pyramidal neuron of the cerebral cortex: morphological and chemical characteristics of the synaptic inputs, *Prog. Neurobiol.* 39 (1992) 563–607.
- [4] A. Destexhe, D. Contreras, M. Steriade, T.J. Sejnowski, J.R. Huguenard, In vivo, in vitro and computational analysis of dendritic calcium currents in thalamic reticular neurons, *J. Neurosci.* 16 (1996) 169–185.

- [5] A. Destexhe, Z. Mainen, T.J. Sejnowski, An efficient method for computing synaptic conductances based on a kinetic model of receptor binding, *Neural Comput.* 6 (1994) 14–18.
- [6] A. Destexhe, Z. Mainen, T.J. Sejnowski, Kinetic models of synaptic transmission, in: C. Koch, I. Segev (Eds.), *Methods in Neuronal Modeling*, MIT Press, Cambridge, MA, 1998, pp. 1–26.
- [7] A. Destexhe, D. Paré, Impact of network activity on the integrative properties of neocortical pyramidal neurons in vivo, *J. Neurophysiol.* 81 (1999) 1531–1547.
- [8] R.J. Douglas, K.A. Martin, D. Whitteridge, An intracellular analysis of the visual responses of neurones in cat visual cortex, *J. Physiol.* 440 (1991) 659–696.
- [9] E.V. Evarts, Temporal patterns of discharge of pyramidal tract neurons during sleep and waking in the monkey, *J. Neurophysiol.* 27 (1964) 152–171.
- [10] M. Hausser, B.A. Clark, Tonic synaptic inhibition modulates neuronal output pattern and spatiotemporal synaptic integration, *Neuron* 19 (1997) 665–678.
- [11] A.L. Hodgkin, A.F. Huxley, A quantitative description of membrane current and its application to conduction and excitation in nerve, *J. Physiol.* 117 (1952) 500–544.
- [12] N. Hô, H. Kröger, A. Destexhe, Consequences of correlated synaptic bombardment on the responsiveness of neocortical pyramidal neurons, *Neurocomputing*, this issue.
- [13] W.R. Holmes, C.D. Woody, Effects of uniform and non-uniform synaptic activation-distributions on the cable properties of modeled cortical pyramidal neurons, *Brain Res.* 505 (1989) 12–22.
- [14] H. Markram, J. Lübke, M. Frotscher, A. Roth, B. Sakmann, Physiology and anatomy of synaptic connections between thick tufted pyramidal neurones in the developing rat neocortex, *J. Physiol.* 500 (1997) 409–440.
- [15] M. Matsumura, T. Cope, E.E. Fetz, Sustained excitatory synaptic input to motor cortex neurons in awake animals revealed by intracellular recording of membrane potentials, *Exp. Brain Res.* 70 (1988) 463–469.
- [16] D. Paré, E. Lebel, E.J. Lang, Differential impact of miniature synaptic potentials on the somata and dendrites of pyramidal neurons in vivo, *J. Neurophysiol.* 78 (1997) 1735–1739.
- [17] D. Paré, E.J. Lang, A. Destexhe, Inhibitory control of somatic and dendritic sodium spikes in neocortical pyramidal neurons in vivo: an intracellular and computational study, *Neuroscience* 84 (1998) 377–402.
- [18] D. Paré, E. Shink, H. Gaudreau, A. Destexhe, E.J. Lang, Impact of spontaneous synaptic activity on the resting properties of cat neocortical neurons in vivo, *J. Neurophysiol.* 79 (1998) 1450–1460.
- [19] M. Rapp, Y. Yarom, I. Segev, The impact of parallel fiber background activity on the cable properties of cerebellar Purkinje cells, *Neural Comput.* 4 (1992) 518–533.
- [20] M. Steriade, F. Amzica, D. Contreras, Synchronization of fast (30–40 Hz) spontaneous cortical rhythms during brain arousal, *J. Neurosci.* 16 (1996) 392–417.
- [21] M. Steriade, F. Amzica, A. Nuñez, Cholinergic and noradrenergic modulation of the slow ( $\sim 0.3$  Hz) oscillation in neocortical cells, *J. Neurophysiol.* 70 (1993) 1384–1400.
- [22] M. Steriade, A. Nunez, F. Amzica, A novel slow ( $< 1$  Hz) oscillation of neocortical neurons in vivo: depolarizing and hyperpolarizing components, *J. Neurosci.* 13 (1993) 3252–3265.
- [23] A.M. Thomson, J. Deuchars, Synaptic interactions in neocortical local circuits: dual intracellular recordings in vitro, *Cerebral Cortex* 6 (1997) 510–522.
- [24] D. Yaeger, E. Deschutter, J. Bower, The role of synaptic and voltage-gated currents in the control of Purkinje cell spiking: a modeling study, *J. Neurosci.* 17 (1997) 91–106.